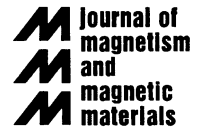




ELSEVIER

Journal of Magnetism and Magnetic Materials 195 (1999) L269–L274



Letter to the Editor

# Perpendicular giant magnetoresistance of $\text{Co}_{91}\text{Fe}_9/\text{Cu}$ exchange-biased spin-valves: further evidence for a unified picture

A.C. Reilly<sup>1</sup>, W. Park, R. Slater, B. Ouaglal, R. Loloe, W.P. Pratt Jr., J. Bass\*

*Department of Physics and Astronomy, Center for Fundamental Materials Research, and NSF MRSEC Center for Sensor Materials, Michigan State University, East Lansing, MI 48824-1116, USA*

Received 10 September 1998; received in revised form 19 November 1998

## Abstract

Measurements are reported of the increase in specific resistance,  $A\Delta R$ , with increasing  $\text{Co}_{91}\text{Fe}_9$  layer thickness in current-perpendicular to the plane (CPP) exchange-biased spin-valves (EBSVs) of  $\text{Co}_{91}\text{Fe}_9$  and Cu. Analysis of these measurements yields a spin anisotropy parameter for  $\text{Co}_{91}\text{Fe}_9$  of  $\beta = 0.65 \pm 0.05$ , and a spin diffusion length of  $l_{\text{sf}}^{\text{CoFe}} = 12 \pm 1$  nm. The value of  $\beta$  agrees reasonably well with those obtained experimentally and theoretically for dilute CoFe alloys, thus providing additional support for a unified picture of spin-polarized transport in CPP-MR and bulk alloys. This value of  $l_{\text{sf}}^{\text{CoFe}}$ , and the previously determined  $l_{\text{sf}}^{\text{P}}$  for Permalloy, scale approximately inversely with the residual resistivities of the two alloys. © 1999 Elsevier Science B.V. All rights reserved.

PACS: 73.40; 72.15; 73.50; 75.50R

Keywords: Giant magnetoresistance; CPP-magnetoresistance; Magnetic multilayers; Spin valve

## 1. Introduction

It is generally accepted that a primary source of giant (G) magnetoresistance (MR) in F/N multilayers (F = ferromagnetic metal, N = nonmagnetic metal) is spin-dependent scattering anisotropy [1,2]. The anisotropy within the F-metal is usually

characterized by a single parameter  $\alpha = (1 + \beta)/(1 - \beta) = \rho^{\downarrow}/\rho^{\uparrow}$ , where  $\rho^{\uparrow,\downarrow}$  are the resistivities for electrons with spins along or opposite to the local magnetization. Since the quantities  $\rho^{\uparrow,\downarrow}$  for the usual current-in-plane (CIP) MR [1,2], the current-perpendicular-to-plane (CPP) MR [3,4], and for bulk F-based alloys [5], each involve different weightings over the Fermi surface, it is not at all obvious that the values of  $\beta$  for the three different cases should be similar. But it is important to determine whether or not they are – i.e., whether  $\beta$  is approximately ‘unified’ [6], both to clearly establish the physical source of  $\beta$  in GMR, and to

\* Corresponding author. Tel.: +1-517-432-1146; fax: +1-517-353-4500.

E-mail address: BASS@PA.MSU.EDU (J. Bass)

<sup>1</sup> Present address: Department of Physics, College of William and Mary, Williamsburg, VA 23187, USA.

see if existing determinations of  $\beta$  in F-based alloys [5], as well as recent calculations [7,8], can give guidance to more effective GMR constituents.

The equations for the CPP-MR are usually simpler than those for the CIP-MR, allowing more direct access to parameters such as  $\beta$  [3,4,9–11]. This simplicity has led us and colleagues [6,12–14] to ask if  $\beta$  for the CPP-MR is similar to that for bulk alloys. Our first test, for  $\text{Ni}_{84}\text{Fe}_{16}$  (Permalloy = Py), gave  $\beta \approx 0.7$  [12], in reasonable agreement with values ( $\beta = 0.76\text{--}0.90$ ) derived experimentally for dilute NiFe alloys [5]. Negative signs of  $\beta$  derived [5] and calculated [7,8] for several Ni- and Co-based alloys were also reproduced in CPP-MR measurements, although the magnitudes from these first experiments [6,13,14] were smaller than expected.

The present study was undertaken to see if the magnitude of the expected positive  $\beta$  for an alloy of a different F-metal, Co, agreed with bulk estimates [5] and calculations [8].  $\text{Co}_{91}\text{Fe}_9$  (hereafter just CoFe) has a simple fcc structure [15], and is of interest for technology because of its low coercivity and good magnetoresistive properties. We report that our newly derived CPP  $\beta = 0.65 \pm 0.05$  is comparable to the independently measured value for dilute bulk CoFe alloys from measurements  $\beta = 0.85 \pm 0.1$  (where we have estimated the uncertainty from the scatter in similar studies [5]). It is also consistent with a calculated value,  $\beta < 0.96$  [8], which should be only an upper bound because of neglect of spin–orbit coupling [7]. The fits to our data also require a finite spin diffusion length (the length over which electrons lose spin-direction memory) in CoFe of  $l_{\text{sf}}^{\text{CoFe}} = 12 \pm 1$  nm. The ratio of this value of  $l_{\text{sf}}^{\text{CoFe}}$  to our previously measured  $l_{\text{sf}}^{\text{Py}} = 5.5 \pm 0.1$  nm for Py [12,16] is approximately the inverse of the ratio of the residual resistivities of the CoFe and Py.

## 2. Samples

To derive CPP-MR parameters, one must be able to reliably produce the two extreme magnetic states on which analysis is based, where the magnetizations,  $\mathbf{M}_i$ , of adjacent F-layers are aligned either parallel (P) or anti-parallel (AP) to each

other. Both states can be achieved using an exchange-biased spin valve (EBSV) [17], where the  $\mathbf{M}_i$  of one F-layer, the ‘pinned’ layer, is held at a high saturation field,  $H_p$ , by exchange-biasing to an adjacent anti-ferromagnetic (AF) layer, while the  $\mathbf{M}_i$  of the other F-layer, the ‘free’ layer, is free to reverse when a lower saturation field,  $H_f$ , is applied. The quantity of primary experimental interest is then the difference in specific resistance (area  $A$  times resistance  $R$ ) between the (higher resistance) AP-state and the (lower resistance) P-state:  $A\Delta R = AR(\text{AP}) - AR(\text{P})$ .

In this paper we present data on: (a) symmetric (free and pinned CoFe layers of equal thickness,  $t_{\text{CoFe}}$ ) and (b) asymmetric (unequal  $t_{\text{CoFe}}$ ) CoFe/Cu EBSVs. Because the pinning field between the F and AF layers decreases with increasing  $t_F$ , there is uncertainty in case (a) about whether the samples achieve an AP state for thick  $t_{\text{CoFe}}$ . To ensure a set of samples with less questionable AP states, in case (b) the pinned  $t_{\text{CoFe}}$  was held fixed at  $t = 6$  nm.

The samples were made by DC triode sputtering in an argon pressure of 2.5 mTorr; details of our growth and measuring procedures are published elsewhere [18]. To achieve a uniform measuring current in the CPP geometry, our EBSVs are sandwiched between two crossed Nb strips of 250-nm thickness and  $\approx 1.1$ -mm width that superconduct at our measuring temperature of 4.2 K. The CoFe target was an alloy purchased from Angstrom Sciences. EDS analysis on films sputtered from this target gave average concentrations of 9% Fe and 91% Co. Our initial samples had the form (Nb/Cu/FeMn/CoFe/Cu/CoFe/Nb), with a 10 nm thick Cu buffer layer on the Nb to ensure proper pinning [16], 8 nm of  $\text{Fe}_{50}\text{Mn}_{50}$ , an adjacent pinned layer of CoFe with  $t_{\text{CoFe}}$  ranging from 3 to 45 nm, 20 nm of Cu (thick enough to minimize exchange coupling between the CoFe layers), and a free layer of CoFe of the same thickness as the pinned one. A later set of samples was grown with the pinned CoFe layer fixed at  $t_{\text{CoFe}} = 6$  nm. A few EBSVs of equal and unequal CoFe layer thickness were also grown with the FeMn deposited after the second CoFe layer. The data for these samples were similar to the rest and are not distinguished. The direction of magnetization of the pinned CoFe layer was set by cooling the EBSV in a magnetic field ( $> 30$  Oe) from

approximately 170°C to just above room temperature [12].

### 3. Data and analysis

Fig. 1 compares complete pinned and unpinning loops for the CPP-resistance,  $R$ , and magnetization,  $M$ , of a symmetric EBSV with  $t_{\text{CoFe}} = 12$  nm. To eliminate contributions from the superconducting Nb,  $M$  was measured with a SQUID magnetometer at 12 K. In an ideal EBSV, the transitions from the P ( $R = \text{minimum}$ , saturated  $|M| = M_s = \text{maximum}$ ) to AP ( $R = \text{maximum}$ ,  $M = 0$ ) states would be sharp and the pinned and unpinning loops would be well separated in field. For  $t_{\text{CoFe}} \leq 20$  nm, we found closely ideal behavior for the CPP-MR (Fig. 1), with well-separated pinned (solid arrows) and unpinning (open arrows) loops, giving well-defined P and AP states. While the transitions for the pinned loop CPP-MR are almost 'square', those for  $M$  are more rounded, with 'tails' [19], suggesting nonideal behavior. The reason for, and significance of, the difference is not known. For  $t_{\text{CoFe}} > 20$  nm, the strength of the exchange biasing decreased to where the pinned and unpinning loops were less well separated, causing uncertainty about attainment of an AP state for the thickest CoFe layers. This problem was mitigated in asymmetric EBSVs, with fixed pinned  $t_{\text{CoFe}} = 6$  nm, which gave CPP-MR and  $M$  loops with nice separation for all free-layer CoFe thicknesses.

Fig. 2 shows the specific resistance,  $A\Delta R$ , versus  $t_{\text{Co}}$  for a series of EBSVs (eight sputtering runs total) with equal CoFe layer thickness (squares and circles). The squares are for CoFe EBSVs made six months prior to those designated by circles, under slightly different sputtering conditions (a different Ar purifier and lower growth temperatures of  $-80$  to  $-20^\circ\text{C}$  rather than our usual  $-30$  to  $+30^\circ\text{C}$  range). To highlight the increase in  $A\Delta R$  due to adding Fe, the triangles in Fig. 2 indicate data for Co/Cu EBSVs [20]. Whereas the Co/Cu data increase monotonically, the CoFe/Cu data level off beyond  $t_{\text{CoFe}} = 30$  nm, suggesting a finite  $t_{\text{sf}}^{\text{CoFe}}$ .

Fig. 3 shows similar data for EBSVs with fixed pinned-layer thickness,  $t_{\text{CoFe}} = 6$  nm.

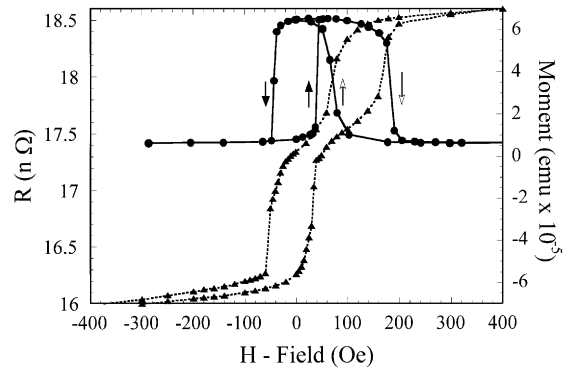


Fig. 1. Hysteresis curves for CPP-resistance,  $R$  (dots, left scale), and magnetization,  $M$  (triangles, right scale), of a CoFe/Cu EBSV with  $t_{\text{CoFe}} = 12$  nm. Arrows on the  $R$  curves indicate direction of field change: solid arrows indicate pinned loop, open arrows, unpinning loop.  $R$  data taken at 4.2 K,  $M$  at 12 K.

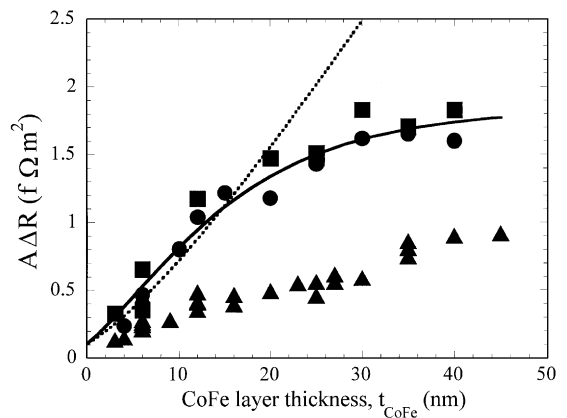


Fig. 2.  $A\Delta R$  (circles and squares) versus  $t_{\text{Co}}$  for symmetric CoFe/Cu EBSVs (equal CoFe thicknesses), with squares indicating early sample runs and circles later ones. Triangles indicate Co/Cu EBSVs for comparison (note that the Co/Cu data increase almost linearly with  $t_{\text{Co}}$ ). Solid curve: VF theory with  $\beta = 0.66$  and  $t_{\text{sf}}^{\text{CoFe}} = 12$  nm. Dotted curve: VF theory with  $\beta = 0.66$  and  $t_{\text{sf}}^{\text{CoFe}} = \infty$ .

For  $t_{\text{sf}}^{\text{CoFe}}$  much longer than the layer thicknesses of our samples, we would expect  $A\Delta R$  to be given by a simple two-current series-resistor equation [3,4] in which the numerator is  $(2\beta\rho_{\text{CoFe}}^*t_{\text{CoFe}} + 2\gamma AR_{\text{CoFe/Cu}}^*)^2$  and the denominator is the AP specific resistance of the sample, consisting of a series sum of the values of  $AR^*$  for each of the interfaces and the values of  $\rho^*t$  for each of the layers between

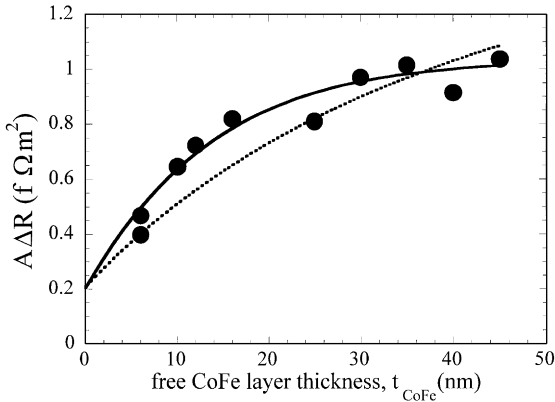


Fig. 3.  $A\Delta R$  (solid circles) versus free-CoFe-layer thickness,  $t_{\text{CoFe}}$ , for asymmetric CoFe/Cu EBSVs with fixed pinned CoFe layer thickness = 6 nm. Solid curve: VF theory with  $\beta = 0.64$  and  $l_{\text{sf}}^{\text{CoFe}} = 12$  nm. Dotted curve: VF theory with  $\beta = 0.64$  and  $l_{\text{sf}}^{\text{CoFe}} = \infty$ .

the Nb contacts. (Here \* indicates the average of values for spin  $\uparrow$  and spin  $\downarrow$ , and  $R_{\text{F}/\text{N}}^{\downarrow}/R_{\text{F}/\text{N}}^{\uparrow} = (1 + \gamma)/(1 - \gamma)$  defines  $\gamma$  for the F/N interface in analogy to the definition of  $\beta$  within the F-metal.) However, we interpret prior measurements of FeMn as indicating that the effective spin-diffusion length in FeMn is short [16]. The Valet–Fert (VF) equations [4] then tell us that contributions ( $AR_{\text{Nb}/\text{CoFe}}$  and  $\rho_{\text{FeMn}}t_{\text{FeMn}}$ ) that lie beyond the FeMn/CoFe interface from the EBSV fall out of the denominator. For long  $l_{\text{sf}}^{\text{CoFe}}$ , we thus expect

$A\Delta R =$

$$\frac{(2\beta\rho_{\text{CoFe}}^*t_{\text{CoFe}} + 2\gamma AR_{\text{CoFe}/\text{Cu}}^*)^2}{AR_{\text{FeMn}/\text{CoFe}} + 2\rho_{\text{CoFe}}^*t_{\text{CoFe}} + \rho_{\text{Cu}}t_{\text{Cu}} + 2AR_{\text{CoFe}/\text{Cu}}^* + AR_{\text{Nb}/\text{CoFe}}}. \quad (1)$$

Eq. (1) predicts that  $A\Delta R$  should grow at least linearly with increasing  $t_{\text{CoFe}}$ . The data of Fig. 2, however, saturate in value beyond  $t_{\text{CoFe}} \sim 30$  nm. This saturation requires a shorter  $l_{\text{sf}}^{\text{CoFe}}$ , necessitating numerical fits to the more complex VF equations for finite  $l_{\text{sf}}^{\text{CoFe}}$  [4].

To minimize adjustability, we fix as many parameters as possible from prior and independent measurements. Prior measurements on Co/Cu multilayers, give  $\rho_{\text{Cu}} = 4.5 \pm 0.5$  nΩm [21]. Since the CoFe layers contain only 9 at% Fe, we take the

CoFe interface to have the same parameters as Co/Cu:  $AR_{\text{CoFe}/\text{Cu}}^* = 0.52 \pm 0.03$  fΩm<sup>2</sup> and  $\gamma_{\text{CoFe}/\text{Cu}} = 0.75 \pm 0.05$  [21]. This assumption receives some support from a similarity of interface resistances for CoFe and Co with Nb and FeMn. Measurements of Nb/Co<sub>91</sub>Fe<sub>9</sub>/Nb sandwiches give  $AR_{\text{Nb}/\text{CoFe}} = 3.5 \pm 0.5$  fΩm<sup>2</sup> (versus  $AR_{\text{Nb}/\text{Co}} = 3.05 \pm 0.5$  fΩm<sup>2</sup> [21]), and measurements of [CoFe/FeMn]<sub>N</sub> multilayers with fixed  $t_{\text{FeMn}} = 8$  nm and  $t_{\text{Co}} = 6$  nm give  $AR_{\text{FeMn}/\text{CoFe}} = 0.95 \pm 0.1$  fΩm<sup>2</sup> (versus  $AR_{\text{FeMn}/\text{Co}} = 0.6 \pm 0.3$  fΩm<sup>2</sup> for Co/FeMn [20]). Combining data on Nb/Cu/Co<sub>91</sub>Fe<sub>9</sub>/Nb sandwiches with van der Pauw measurements gives  $\rho_{\text{CoFe}} = 70 \pm 10$  nΩm. The only adjustable parameters are those for bulk CoFe:  $\beta$  and  $l_{\text{sf}}^{\text{CoFe}}$ .

To not bias each by the other, the data of Figs. 2 and 3 were fit separately, with  $\chi^2$  minimized using the ‘best’ non-adjustable parameters listed above. These fits are the solid curves in Figs. 2 and 3. Given the uncertainties in the non-adjustable parameters, the agreement in values of  $\beta$  and  $l_{\text{sf}}^{\text{CoFe}}$  is surprisingly good:  $\beta = 0.66 \pm 0.04$ ,  $l_{\text{sf}}^{\text{CoFe}} = 12 \pm 1$  nm for the symmetric EBSVs and  $\beta = 0.64 \pm 0.05$ ,  $l_{\text{sf}}^{\text{CoFe}} = 12 \pm 1$  nm for the asymmetric ones. The differences are well within the separate uncertainties. Possible sources for the differences include: greater sensitivity of the asymmetric EBSVs to  $AR_{\text{FeMn}/\text{CoFe}}$  for the interface between the FeMn and CoFe; the aforementioned possible lack of achievement of an AP state for the thickest symmetric EBSVs; and/or the scatter in the symmetric EBSV data for the different sets of samples separated by six months. To conclude this part of the discussion, we note that combining the parameters that give the solid curves in Figs. 2 and 3, with prior measurements of  $AR_{\text{Nb}/\text{FeMn}} = 1.0 \pm 0.4$  fΩm<sup>2</sup> and  $\rho_{\text{FeMn}} = 875 \pm 50$  nΩm [16], yields predicted curves that fall in the middle of the (rather scattered) data for  $AR(\text{P})$  and  $AR(\text{AP})$  that were used to obtain  $A\Delta R$ . Our analysis is, thus, internally consistent.

For comparison, the dotted curves in Figs. 2 and 3 indicate the VF ‘predictions’ for  $A\Delta R$  with the same parameters, except with  $l_{\text{sf}}^{\text{CoFe}} = \infty$ . These curves serve two purposes. First, they show that the data do not display the forms expected for  $l_{\text{sf}}^{\text{CoFe}} = \infty$  (we have checked that simply adjusting

$\beta$  will not let us fit the data). Second the data show an at-first surprising behavior: for small  $t_{\text{CoFe}}$ , reducing  $l_{\text{sf}}^{\text{CoFe}}$  with all other parameters fixed increases  $A\Delta R$  – a decrease in  $l_{\text{sf}}^{\text{CoFe}}$  is usually expected to decrease  $A\Delta R$  [22]. This unusual increase is due to an interesting property of the VF equations noted above – when  $t_{\text{CoFe}}$  becomes longer than  $l_{\text{sf}}^{\text{CoFe}}$ , only those terms in the denominator of Eq. (1) within  $l_{\text{sf}}^{\text{CoFe}}$  of the CoFe/Cu interfaces remain active. The denominator of Eq. (1) reduces to the sum of terms from only the Cu layer in the middle of the EBSV, the two CoFe/Cu interfaces, and those parts of the CoFe layers within  $l_{\text{sf}}^{\text{CoFe}}$  of the CoFe/Cu interfaces.

Finally, we checked our parameters by using them to predict, without adjustment,  $A\Delta R$  for EBSVs of the form (FeMn/CoFe/Cu/Py), with  $t_{\text{Py}} = 6$  nm. Combining pinning with the innately higher  $H_s$  of CoFe, should give good AP and P states. Fig. 4 compares the predicted curve with the values of  $A\Delta R$  for samples with  $5 \text{ nm} \leq t_{\text{CoFe}} \leq 20$  nm, all of which had generally satisfactory AR loops. Most of the data fall close to the predicted curve.

Lastly, we turn to  $l_{\text{sf}}^{\text{CoFe}}$ . VF theory gives the relation [22]

$$l_{\text{sf}} = \sqrt{(\lambda_e \lambda_{\text{sf}})/6}, \quad (2)$$

where  $\lambda_e$  is the usual mean-free-path for momentum transfer and  $\lambda_{\text{sf}}$  is the mean-free-path for

spin-memory loss. Fert and colleagues [22,23] have suggested that  $\lambda_{\text{sf}}$  might often be approximated as proportional to  $\lambda_e$  which, in turn, is inversely proportional to the residual resistivity,  $\rho_0$ . If so, we expect  $l_{\text{sf}} \propto (1/\rho_0)$ . Our derived ratio of  $l_{\text{sf}}^{\text{CoFe}}/l_{\text{sf}}^{\text{Py}} = (12 \pm 1 \text{ nm})/(5.5 \pm 1 \text{ nm}) = 2.2 \pm 0.5$  is consistent with the ratio  $\rho_{\text{Py}}/\rho_{\text{CoFe}} = (123 \pm 40 \text{ n}\Omega\text{m})/(70 \pm 10 \text{ n}\Omega\text{m}) = 1.8 \pm 0.8$ . The source of these relatively short values of  $l_{\text{sf}}$  is not yet known. Dubois et al. [23] propose spin-orbit scattering, but independently measured spin-orbit relaxation times with which to test their proposal are not yet available.

#### 4. Conclusion

We report the first CPP-MR measurements of  $\text{Co}_{91}\text{Fe}_9/\text{Cu}$  EBSVs. Data for both symmetric and asymmetric EBSVs can be fit with the VF theory for finite spin diffusion length, yielding  $\beta = 0.65 \pm 0.05$  and  $l_{\text{sf}}^{\text{CoFe}} = 12 \pm 1$  nm. This value of  $\beta$  is close enough to those obtained from measurements on dilute CoFe alloys [5] and a recent calculation [8] to provide additional support for the proposed ‘unified’ picture of  $\beta$  [6]. The derived parameters are able to predict reasonably well, without adjustment, the values of  $A\Delta R$  for CPP-EBSVs of CoFe with Py. Our inferred spin-diffusion length for CoFe,  $l_{\text{sf}}^{\text{CoFe}} = 12 \pm 1$  nm, and our previously determined one for Py,  $l_{\text{sf}}^{\text{Py}} = 5.5 \pm 1$  nm, scale approximately inversely with the residual resistivities of CoFe and Py. This study illustrates the power of using CPP-EBSVs for determining important transport parameters.

#### Acknowledgements

This work was supported in part by NSF DMR grants 94-23795 and 94-00417 (MRSEC), the MSU CFMR and CSM, and Ford Research Laboratory.

#### References

- [1] M.N. Baibich, J.M. Broto, A. Fert, F. Nguyen Van Dau, F. Petroff, P. Etienne, G. Creuzet, A. Friederich, J. Chazelas, Phys. Rev. Lett. 61 (1988) 2472.

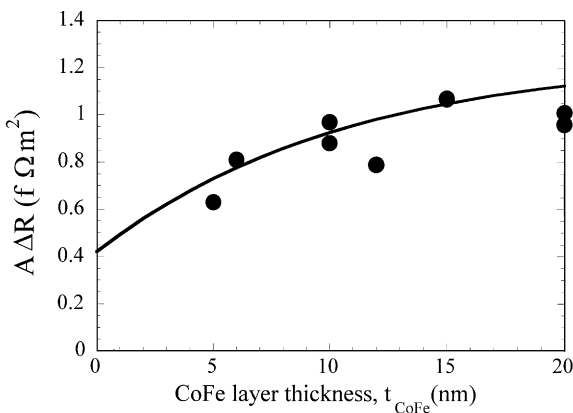


Fig. 4.  $A\Delta R$  versus  $t_{\text{CoFe}}$  for CoFe/Cu/Py EBSVs, with constant  $t_{\text{Py}} = 6$  nm. Solid line: calculation from VF theory with the fixed parameters listed in the text.

- [2] P.M. Levy, in: H. Ehrenreich, D. Turnbull (Eds.), *Solid State Physics*, Vol. 47, Academic Press, New York, 1994, p. 367.
- [3] S.F. Lee, W.P. Pratt Jr., Q. Yang, P. Holody, R. Loloee, P.A. Schroeder, J. Bass, *J. Magn. Magn. Mater* 118 (1993) L1.
- [4] T. Valet, A. Fert, *Phys. Rev. B* 48 (1993) 7099.
- [5] I.A. Campbell, A. Fert, in: E.P. Wohlfarth (Ed.), *Ferromagnetic Materials*, Vol. 3, North Holland, Amsterdam, 1982, p. 747.
- [6] S.Y. Hsu, A. Barthelemy, P. Holody, R. Loloee, P.A. Schroeder, A. Fert, *Phys. Rev. Lett.* 78 (1997) 2652.
- [7] I. Mertig, R. Zeller, P.H. Dederichs, *Phys. Rev. B* 47 (1993) 16178.
- [8] I. Mertig, R. Zeller, P.H. Dederichs, in: J.S. Faulkner, R. Jordan (Eds.), *Metallic Alloys: Experimental and Theoretical Perspectives*, Kluwer Academic Publishers, Dordrecht, 1994, p. 423.
- [9] S. Zhang, P.M. Levy, *J. Appl. Phys.* 69 (1991) 4786.
- [10] M.A.M. Gijs, G.E.W. Bauer, *Adv. Phys.* 46 (1997) 285.
- [11] J. Bass, W.P. Pratt Jr., P.A. Schroeder, *Comm. Condens. Matter. Phys.* 81 (1998) 223.
- [12] S.D. Steenwyk, S.Y. Hsu, R. Loloee, J. Bass, W.P. Pratt Jr., *J. Magn. Magn. Mater.* 170 (1997) L1.
- [13] C. Vouille, A. Fert, A. Barthelemy, S.Y. Hsu, R. Loloee, P.A. Schroeder, *J. Appl. Phys.* 81 (1997) 4573.
- [14] P.A. Schroeder, P. Holody, R. Loloee, C. Vouille, A. Barthelemy, A. Fert, S.Y. Hsu, *J. Magn. Magn. Mater.* 177-181 (1998) 1464.
- [15] M. Hanson, in: K. Anderko (Ed.), *Constitution of Binary Alloys*, McGraw-Hill, New York, 1958.
- [16] W.P. Pratt Jr., S.D. Steenwyk, S.Y. Hsu, W.-C. Chiang, A.C. Schaefer, R. Loloee, J. Bass, *IEEE Trans. Mag.* 33 (1997) 3305.
- [17] B. Dieny, V.S. Speriosu, S. Metin, S.S.P. Parkin, P. Baumgart, D.R. Wilhoit, *J. Appl. Phys.* 69 (1991) 4774.
- [18] S.F. Lee, Q. Yang, P. Holody, R. Loloee, J.H. Hetherington, S. Mahmood, B. Ikegami, K. Vigen, L.L. Henry, P.A. Schroeder, W.P. Pratt Jr., J. Bass, *Phys. Rev. B* 52 (1995) 15426 and references therein.
- [19] S. Steenwyk, S.Y. Hsu, R. Loloee, J. Bass, W.P. Pratt Jr., *J. Appl. Phys.* 81 (1997) 4011.
- [20] A.C. Reilly, W.-C. Chiang, W. Park, S.Y. Hsu, R. Loloee, S. Steenwyk, W.P. Pratt Jr., J. Bass, *IEEE Trans. Magn.* 34 (1998) 939.
- [21] W.P. Pratt Jr., Q. Yang, L.L. Henry, P. Holody, W.-C. Chiang, P.A. Schroeder, *J. Appl. Phys.* 79 (1996) 5811.
- [22] A. Fert, J.L. Duvail, T. Valet, *Phys. Rev. B* 52 (1995) 6513.
- [23] S. Dubois, L. Piraux, J.M. George, K. Ounadjela, R. Ferre, J.L. Duvail, A. Fert, Submitted for publication.